



Investigation of Splat Curling up in Thermal Spray Coatings

Minxia Xue, Sanjeev Chandra, and Javad Mostaghimi

(Submitted February 28, 2006; in revised form April 25, 2006)

Peer Reviewed

The curling up of the edges of splats of molten metal deposited on a cold substrate was investigated both experimentally and numerically. An analytical model, based on mismatch of thermal expansion between the splat and substrate, was developed to calculate the deformation of splats after curling up. The curling-up angle was measured from both millimeter-sized splats of aluminum alloy and bismuth and plasma-sprayed nickel particles. The curling-up angles were predicted using both the analytical model and a numerical code and were found to agree reasonably well with experimental measurements.

Keywords curling up, splat deformation, thermal expansion, thermal spray coating, thermal stresses

1. Introduction

Curling up at the edge of splats is frequently observed in thermal spray coatings and is one of the main sources of coating porosity. The degree of curling up is affected by several factors, such as stresses generated by mismatch of thermal expansion coefficient at the coating interface, surface tension of the liquid splat, surface roughness, and remelting. Because the mechanism of the curling up is extremely complicated, few attempts have been made to quantify it.

Fukanuma (Ref 1) proposed a physical and mathematical model for the production of porosity by considering deformation of a molten particle during thermal spray coating processes. He observed that most pores exist at the periphery of splats, starting at ~ 0.6 times the splat radius (R) from its center. Zhao et al. (Ref 2) presented an experimental study of liquid droplet impinging upon a substrate. Droplet impact was characterized by spread, recoil, and oscillations. Spreading and recoiling motions depended upon the initial velocity and droplet properties. Sobolev and Guilemany (Ref 3) derived a set of analytical formulae to describe the pressure distribution in a flattening droplet along the droplet-substrate interface during thermal spraying. Droplet-substrate microadhesion and coating porosity along the radius were shown to depend on the ratio of the pressure developed upon impact to the capillary pressure. Cirolini et al. (Ref 4) developed a model for the deposition of a thermal barrier plasma-sprayed coating assuming that curling was caused by the tem-

perature drop across the splat when the solidification front just reached the top. Wroblewski et al. (Ref 5) developed a two-dimensional, finite-element model based on an enthalpy formulation to simulate a splat solidifying on a rough substrate. Remelting was studied because it is indicative of local heat-transfer conditions and might explain the observed coating properties. The presence of roughness promoted substrate remelting at conditions under which no remelting was observed for a smooth surface, suggesting that substrate roughness is an important parameter to include in splat-solidification studies.

Curl-up location and magnitude depend on coating materials and impact conditions. To simulate the thermal spray coating process, the mechanism of curling up needs to be understood. In this study, cross sections of splats obtained from experiments were examined. A numerical code was used to simulate heat transfer during splat cooling, calculate stress distributions in the splat and substrate and to determine the degree of curling up. A simple analytical model was developed to predict the curling-up angle as a function of impact parameters and material properties.

2. Experimental Investigations

Heichal and Chandra (Ref 6) studied experimentally the normal impact of large (~ 4 mm diameter) aluminum alloy 380 (85.5% Al, 8.5% Si, 4% Cu, 2% Fe) and bismuth (99% pure) droplets falling under their own weight and landing with 1-3 m/s velocity on a steel substrate. The initial temperature of aluminum alloy droplets was 630 °C. The solidus temperature of the

NOMENCLATURE

<i>h</i>	splat thickness at the maximum extent
<i>D</i>	droplet diameter
<i>s</i>	length difference
<i>V</i>	velocity
α	thermal expansion coefficient
θ	curl-up angle
<i>d</i>	droplet
<i>s</i>	splat
<i>0</i>	initial
<i>f</i>	spreading finishes

This article was originally published in *Building on 100 Years of Success, Proceedings of the 2006 International Thermal Spray Conference* (Seattle, WA), May 15-18, 2006, B.R. Marple, M.M. Hyland, Y.-Ch. Lau, R.S. Lima, and J.Voyer, Ed., ASM International, Materials Park, OH, 2006.

Minxia Xue, Sanjeev Chandra, and Javad Mostaghimi, Center for Advanced Coating Technologies Department of Mechanical and Industrial Engineering, University of Toronto, 5 King's College Road, Toronto, Ontario, M5S 3G8, Canada. Contact e-mail: mxue@mie.utoronto.ca.

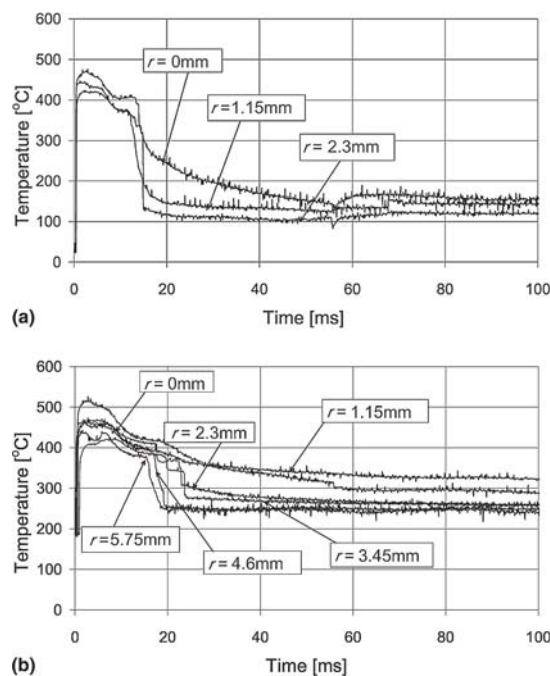


Fig. 1 Substrate surface temperature histories at different radial locations after deposition of an aluminum splat on an H13 tool steel substrate with $R_a = 5 \mu\text{m}$: (a) $T_w = 25^\circ\text{C}$; (b) $T_w = 200^\circ\text{C}$

aluminum 380 alloy is 538°C , and its liquidus temperature is 593°C . For purposes of simulation, a constant melting temperature of 570°C was assumed. Bismuth droplets had an initial temperature of 331°C , and the melting point of bismuth is 271°C .

Temperature histories at different radial locations on the substrate surface under impact droplets were recorded using an array of thin-film thermocouples for a range of substrate temperatures and surface roughness. The experimental method and measurements were reported in detail by Heichal and Chandra (Ref 6). Figure 1 shows typical measurements of substrate surface temperature histories at different radial locations under an aluminum 380 splat with average surface roughness (R_a) $5 \mu\text{m}$ and initial substrate temperature (T_w) equal to either (a) 25°C or (b) 200°C . Up to six thermocouples were placed under each splat, at intervals of 1.15 mm starting from the splat center. The radial location of each thermocouple (r) is indicated in the figures. Immediately after impact ($t = 0$), the temperature rises very rapidly (in $<3 \text{ ms}$) to $\sim 500^\circ\text{C}$. The substrate begins to cool, until the thermocouple farthest from the center (labeled $r = 2.3 \text{ mm}$ in Fig. 1a) shows a sudden temperature drop at approximately $t = 15 \text{ ms}$. This was followed by a temperature drop at the second ($r = 1.15 \text{ mm}$) thermocouple. Similar sudden temperature drops can be seen for the six thermocouples in Fig. 1(b), starting at the outermost edge and progressing inward. The sudden temperature drop indicates the instant of curling up, when the splat loses contact with the substrate, leading to rapid substrate cooling.

Observation of cooling curves shows that, as surface temperature is increased, the time at which curling up occurs is delayed (compare Fig. 1a and b). Curling up starts earlier as surface roughness increases and progresses further toward the splat center.

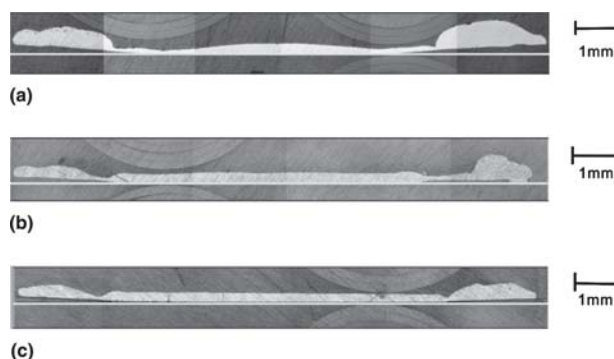


Fig. 2 Cross sections through the centers of aluminum alloy 380 splats on a nonoxidized steel substrate surface, $R_a = 0.5 \mu\text{m}$: (a) $T_w = 30^\circ\text{C}$; (b) $T_w = 100^\circ\text{C}$; and (c) $T_w = 200^\circ\text{C}$

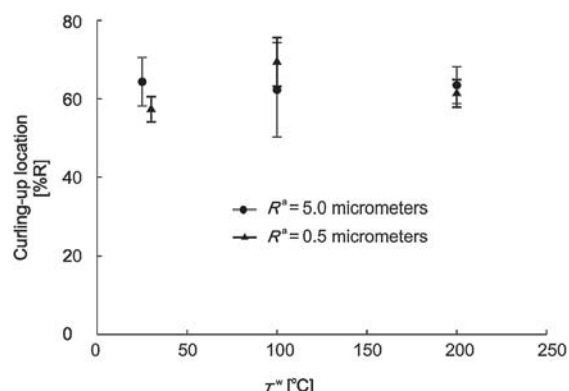


Fig. 3 Mean values of curl-up location with different substrate temperatures and surface roughness for aluminum alloy splats deposited on a nonoxidized steel substrate

Splats obtained from the experiments of Heichal and Chandra (Ref 6) were cross-sectioned for this study and photographed using an optical microscope. Figure 2 shows cross sections of splats formed by 3.92 mm diameter aluminum alloy 380 droplets at 630°C after they had impacted on tool steel surfaces at temperatures of (a) 30°C , (b) 100°C , and (c) 200°C with 3 m/s velocity. The location of the substrate is indicated by a white line in each photograph. Curling up at the edges of splats can be clearly seen. A line was drawn through the point of detachment, tangential to the bottom surface of the splat. The angle between this line and the plane of the substrate was defined as the curl-up angle.

Figures 3 and 4 show the mean values of curl-up location and curl-up angle with different substrate temperatures for average surface roughness of 0.5 and $5.0 \mu\text{m}$. Each data point represents the average of four samples. The error bars show the standard deviations. Splat curl up started at a radial location from the splat center equal to 0.6 – 0.7 times the splat radius, R , irrespective of substrate temperature (Fig. 3). Average curl-up angle appeared to decrease slightly with increasing substrate temperature, but the scatter in the data was too large to draw any firm conclusions (Fig. 4). Substrate roughness in the range 0.5 – $5 \mu\text{m}$ had no measurable effect on curl-up location or angle.

Figure 5 shows typical cross sections of bismuth splats on a stainless steel 303 substrate for impact velocities (a) 1 and (b) 3

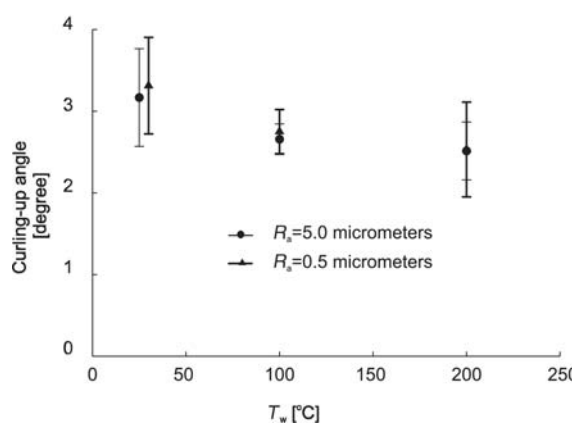


Fig. 4 Mean values of curl-up angle with different substrate temperatures and surface roughness for aluminum alloy splats deposited on a nonoxidized steel substrate

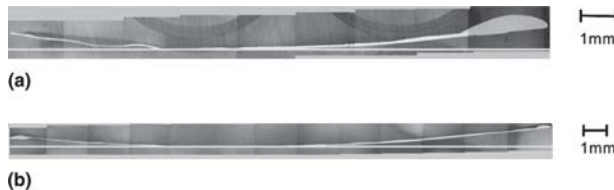


Fig. 5 Cross sections through centers of bismuth splats on stainless steel 303 substrates with initial surface temperature 25 °C and $R_a = 0.06 \mu\text{m}$: (a) $V_0 = 1 \text{ m/s}$; (b) $V_0 = 3 \text{ m/s}$

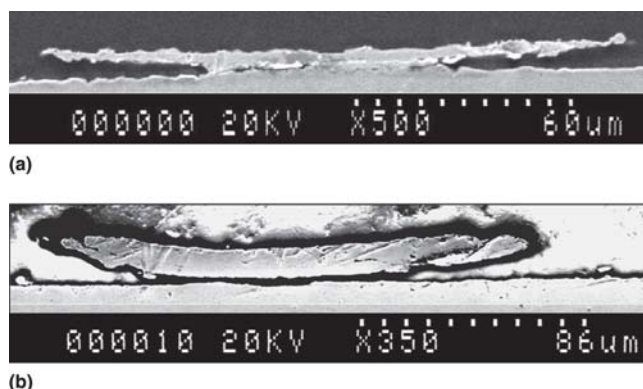


Fig. 6 Cross sections through centers of nickel splats on a stainless steel 303 substrate with initial surface temperature 400 °C: (a) 0.38 of the splat radius is bonded; (b) 0.49 of the splat radius is bonded

m/s. The substrate initial temperature was 25 °C, and surface roughness was 0.06 μm. Initial droplet diameter was 4.0 mm. The location at which curling up started was smaller than with the aluminum alloy splats: at impact velocity of 1 m/s, curling up began at $0.33R$ and the curl-up angle was 3.4°; for 3 m/s impact velocity, curling up began at $0.36R$ and the curl-up angle was 4°.

Figure 6 shows two cross sections through two splats formed by plasma spraying nickel powders onto a stainless steel 303 substrate initially at 400 °C. In Fig. 6(a), the splat starts curling up at about $0.38R$, and the curl-up angle was measured to be 5.5°.

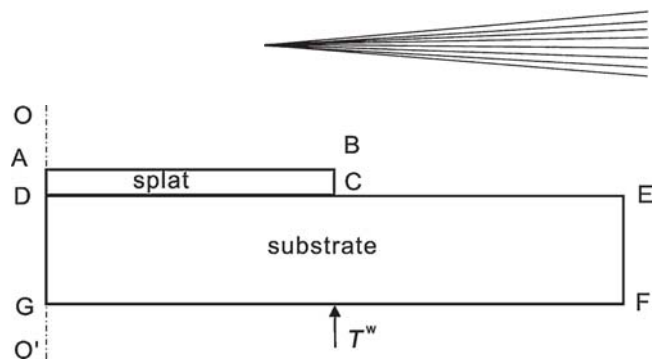


Fig. 7 Schematic of the model used to simulate heat transfer and residual stresses in the splat and substrate

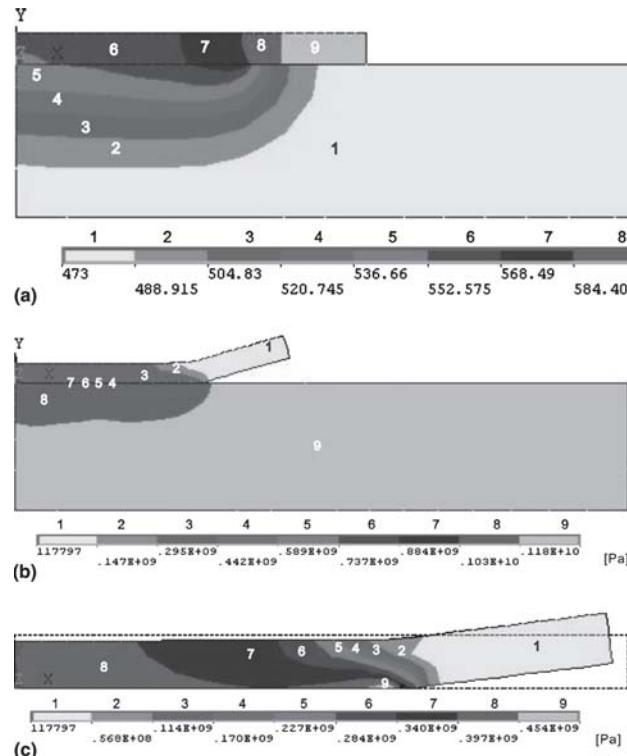


Fig. 8 Typical simulation results of the temperature distribution and structural deformation of the aluminum alloy splat and tool steel substrate at time 0.1 s (interface between the splat and the substrate is partly bonded according to experimental measurement): (a) temperature distribution; (b) stress distribution; (c) magnified stress distribution and deformation of the splat (temperatures are in K; stresses are in Pa)

In Fig. 6(b), the splat starts curling up at about $0.49R$, and the curl-up angle was measured to be 6.5°. Again, a greater radius of bonding of the splat to the substrate results in a larger curl-up angle.

3. Numerical Simulations

A commercial finite-element code (ANSYS 10.0 University Intermediate, ANSYS Inc., Canonsburg, PA) was used to simulate heat transfer during cooling down of the splat and the substrate and to examine splat deformation caused by thermal stresses. Axisymmetric 2-D coordinates were used to define the geometry of the splat and substrate.

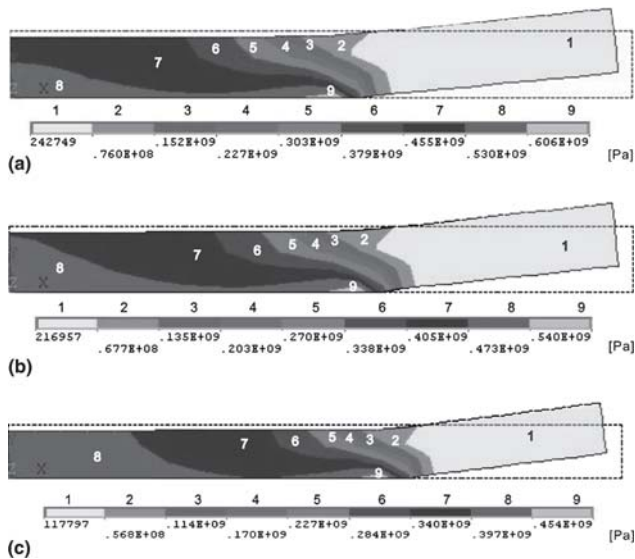


Fig. 9 Simulated curling-up angle with different substrate temperatures and splat sizes from experiments at 0.1 s: (a) $T_w = 30$ °C, curl-up angle = 7°; (b) $T_w = 100$ °C, curl-up angle = 6.5°; (c) $T_w = 200$ °C, curl-up angle = 6.2° (stresses are in Pa; dotted lines show the initial position of the splat)

Figure 7 shows a schematic diagram of the model. All surfaces exposed to air were assumed to be adiabatic. The bottom of the substrate (line FG) was assumed to be isothermal and was set to the initial substrate temperature. The initial temperature of the bulk splat was set to its melting temperature. The initial substrate temperature was prescribed. Heat transfer between the splat and substrate was started at time $t = 0$. The system was assumed to be thermoelastic.

Simulations were done for some of the cases observed experimentally. Figure 8 shows results from a simulation done for the aluminum alloy splat of Fig. 2(c) on the steel substrate, with initial substrate temperature $T_w = 200$ °C. The splat radius was 5.67 mm, and the splat was bonded to the substrate over a distance equal to $0.65R$. The splat thickness, measured at the edge of the splat, was 0.5 mm. The substrate radius was set to twice that of the splat (12 mm), and its thickness was 2.5 mm. The substrate was assumed to be perfectly rigid, so thermal stresses in the splat, and consequently curl-up angle values, would be larger than those expected in reality. The aim, though, was to study trends rather than accurately predict actual values.

In Fig. 8, the splat was cooled down from an initial temperature of 570 °C. Splat boundaries were free to move except at the interface where perfect bonding between the splat and substrate were assumed over a distance equaling 0.65 of the splat radius. Figure 8(a) shows the temperature distribution after the splat and the substrate had been cooling for 0.1 s. Note that the temperature variation in the splat is almost entirely radial; there is a negligible temperature difference between the top and bottom of the splat at a given radial location. Figure 8(b) shows the corresponding thermal stress distribution at $t = 0.1$ s and the deformation along the periphery of the splat. Thermal stresses are created because the bonded portion of the splat does not shrink, as it is attached to the rigid substrate, while the upper surface of the splat contracts as it cools. The splat curled up due to thermal

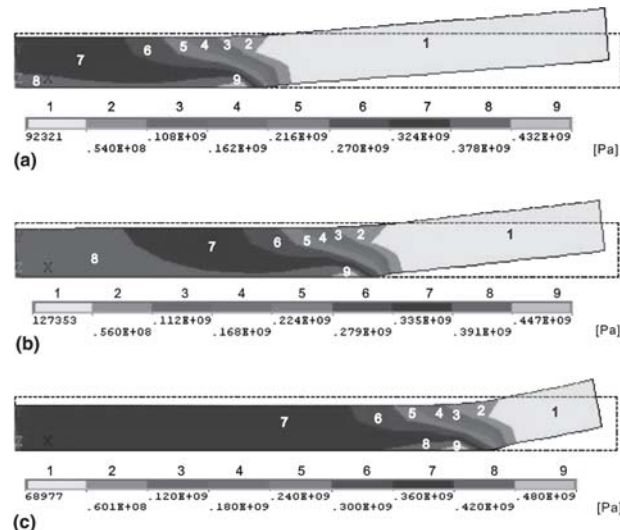


Fig. 10 Simulated curling-up angle with different assigned curling-up locations at 0.1 s: (a) starts curling at $0.4R$, curl-up angle = 4°; (b) starts curling at $0.6R$, curl-up angle = 5.5°; (c) starts curling at $0.8R$, curl-up angle = 10° (stresses are in Pa; dotted lines show the initial position of the splat)

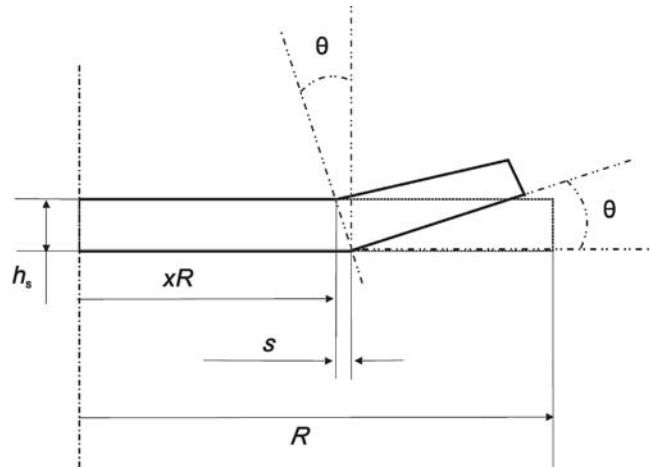


Fig. 11 Schematic of the analytical model of splat curling-up angle

stresses, with the unbonded portion detaching from the substrate. Figure 8(c) shows a larger view of the splat alone, giving a detailed stress distribution. Dotted lines show the initial splat position. The detached portion of the splat was stress free, and the curling-up angle was ~6.2° in this case.

Figure 9 shows simulation results of three splats with different substrate initial temperatures corresponding to the three splats of Fig. 2. When the substrate initial temperature increased from 30 to 200 °C, the curling-up angle decreased from 7 to 6.2°. Simulations showed that the curl-up angle decreases with higher substrate temperature. Values obtained from simulations were somewhat greater than those seen in experiments. This may have been due to the fact that the substrate was not perfectly rigid, as assumed in the authors' simulation.

Figure 10 shows splat shapes after 0.1 s of heat transfer be-

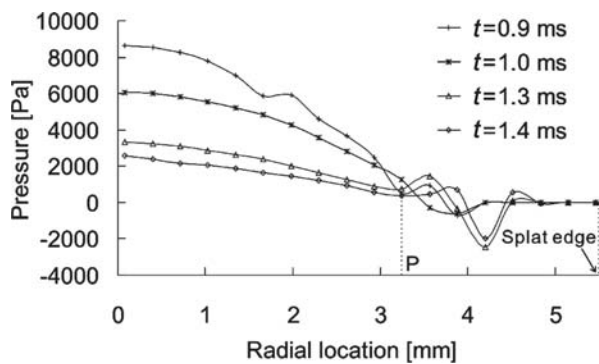


Fig. 12 Simulated radial pressure distribution at four different instants during impact of a 4.0 mm diameter aluminum alloy droplet spreading on a tool steel substrate with $R_a = 0.5 \mu\text{m}$, $V_0 = 3 \text{ m/s}$, and $T_w = 30^\circ\text{C}$

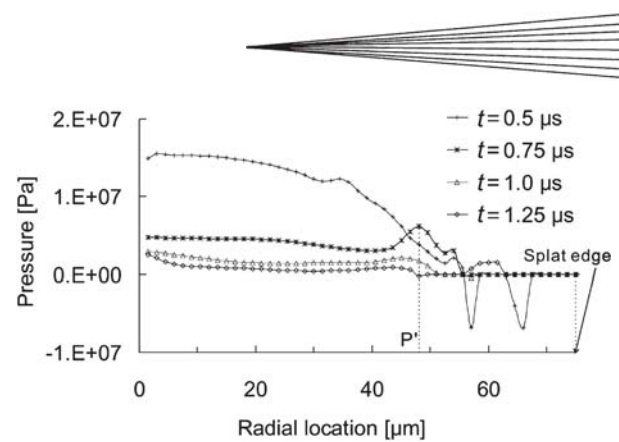


Fig. 13 Simulated radial pressure distribution at four different instants during impact of a 61 μm diameter thermally sprayed nickel droplet spreading on a stainless steel substrate with $R_a = 0.5 \mu\text{m}$, $V_0 = 72 \text{ m/s}$, and $T_w = 400^\circ\text{C}$

Table 1 Measured and predicted (Eq 3) curling-up angles with typical splat and substrate combinations

Splat/substrate	R	h_s	x	$T_w, ^\circ\text{C}$	$\theta_{\text{predict}}, \text{deg}$	$\theta_{\text{measure}}, \text{deg}$
Aluminum alloy/tool steel	5.61 mm	0.61 mm	0.56	30	3.2	3.8
	5.64 mm	0.60 mm	0.60	100	3.0	2.8
	5.67 mm	0.50 mm	0.65	200	3.1	2.5
Bismuth/steel	7.9 mm	0.2 mm	0.33	25	2.9	3.4
	11.9 mm	0.1 mm	0.36	25	8.0	4.0
Nickel/stainless steel	82 μm	4 μm	0.38	400	6.1	5.5
	93 μm	8 μm	0.49	400	4.4	6.5

tween the splat and the substrate. The splat size was the same as the splat in Fig. 8, but the portion of splat radius bonded to the substrate was varied from 0.4 to 0.8R in steps of 0.2R, where R is the splat radius. Other conditions being the same, curling-up angle increases with the attached area.

Further simulations revealed that increasing either the thermal expansion coefficient or Young's modulus of the splat enhanced thermal stresses and therefore the curl-up angle.

4. Analytical Model of Curl-up Angle

After the droplet impacts on the surface, it spreads across the surface and solidifies. As it then cools down to room temperature, it shrinks. If a portion of the bottom is bonded to the substrate, it cannot shrink, but the upper surface of the splat is free to contract, so that stresses are created in the splat. To relieve these stresses, the unbonded portion of the splat, along its periphery, curls up. Note that a splat that is not bonded to the substrate will not curl but will instead contract uniformly along both faces.

Consider a splat bonded over a fraction x of its radius R to the substrate (Fig. 11). The splat has thermal expansion coefficient α , and it cools from the initial droplet temperature T_d to the substrate temperature T_w by the amount $\Delta T = T_d - T_w$.

Because the bonded portion of the splat has a fixed size, this creates a difference in length, s , between the top and bottom surfaces of the unbonded portion of the splat. The top of the splat will contract $xR\alpha\Delta T$ more than the bottom so that:

$$s = xR\alpha\Delta T \quad (\text{Eq 1})$$

Geometrically (Fig. 11),

$$\tan \theta = s/h_s \quad (\text{Eq 2})$$

Substituting Eq 2 into Eq 1, for a splat of radius R and thickness h_s , the curl-up angle will be:

$$\theta = \arctan\left(\frac{xR\alpha\Delta T}{h_s}\right) \quad (\text{Eq 3})$$

Table 1 shows comparisons for predictions from Eq 3 against the experimental measurements. Here, θ_{measure} is the curling-up angle measured experimentally, while θ_{predict} is the predicted curling-up angle using Eq 3 with the splat sizes and the bonded fractions from experiments. The melting temperature of the droplet material was applied as the initial droplet temperature. As substrate temperature is increased, ΔT decreases; consequently, the curl-up angle also becomes smaller. Figure 4 appears to show a similar trend, although the scatter in the data was too large to draw firm conclusions. In general, there is reasonable agreement between prediction and theory.

In the calculations of Table 1, the bonded fraction of the splat radius, x , was measured experimentally. However, in a predictive model, it is necessary to know this value a priori. Little is presently understood about how the bonded fraction varies with process parameters. However, experimental evidence has shown that the bonded fraction seems fairly constant: Fukanuma (Ref 1) observed that most pores in thermal spray coatings exist at the periphery of splats, starting at about 0.6R from its center. Ghaffouri Azar et al. (Ref 7) assumed in their model of thermal spray coating formation that all splats curl up at 0.6R.

Adhesion between splats and the substrate is largely mechanical, when high pressure in the impacting droplet drives liquid into surface crevices where it freezes and forms interlocking connections. Good bonding would be expected to occur over the

region of highest pressure in the droplet. Pressure distributions inside impacting droplets can be accurately calculated using a numerical model (Ref 8).

Figure 12 shows the simulated radial pressure distribution across the splat-substrate interface at four different instants during the spreading of a 4 mm diameter aluminum alloy droplet with initial velocity of 3 m/s on an H13 tool steel substrate with temperature $T_w = 30^\circ\text{C}$ and surface roughness $R_a = 0.5 \mu\text{m}$. Gauge pressures are calculated; negative pressures are those lower than the ambient air, and these occur when the free surface of the droplet is concave (i.e., it has a negative curvature) (Ref 8). The interfacial pressure decreases very rapidly during droplet spreading. Droplet spreading time was ~ 3.0 ms, and within half that time, the peak pressure dropped by $\sim 75\%$. At all times, the pressure dropped to almost zero at the same radial location at 3.2 mm (labeled P in Fig. 12). Because the maximum splat radius was 5.5 mm, this location was at $\sim 0.6R$, which agrees with the measurements of Fig. 3 and offers support for Fukanuma's observation (Ref 1).

Figure 13 shows calculated pressure distributions inside a 61 μm nickel droplet thermally sprayed with 72 m/s initial impact velocity onto a stainless steel substrate at temperature $T_w = 400^\circ\text{C}$ and surface roughness $R_a = 0.5 \mu\text{m}$, the same conditions as for the nickel splats shown in Fig. 6. The final splat radius in this simulation was 75 μm , and droplet impact time was 2 μs . Pressure curves dropped to zero at $\sim 50 \mu\text{m}$, which was $0.66R$. In reality, the exact length of the splat adhering to the substrate will also depend on surface conditions, such as roughness and cleanliness. However, in the absence of other information, $x = 0.6$ appears to be a reasonable guess.

5. Summary and Conclusions

In this paper, curling up of splats formed by impact of molten metal drops has been investigated both experimentally and nu-

merically. Splat curling up is assumed to be entirely due to shrinkage of splats as they cool from a high initial temperature to the substrate temperature. If the central portion of the splat is attached to the substrate, it cannot contract; however, the upper surface shrinks, which causes the edges to curl up. The splat curl-up angle increases with the area of the splat bonded to the substrate and decreases with higher substrate temperature. Increasing the thermal expansion coefficient or the Young's modulus of the splat increases the curl-up angle. A simple analytical model can be used to estimate the magnitude of the curl-up angle.

References

1. H. Fukanuma, A Porosity Formation and Flattening Model of an Impinging Molten Particle in Thermal Spray Coatings, *J. Therm. Spray. Technol.*, 1994, **3**(1), p 33-44
2. Z. Zhao, D. Poulikatos, and J. Fukai, Heat Transfer and Fluid Dynamics During the Collision of a Liquid Droplet on a Substrate. II. Experiments, *Int. J. Heat Mass Transfer*, 1996, **39**(13), p 2791-2802
3. V.V. Sobolev and J.M. Guilemany, Droplet-Substrate Impact Interaction in Thermal Spraying, *J. Mater. Lett.*, 1996, **28**, p 331-335
4. S. Cirolini, J.H. Harding, and G. Jacucci, Computer Simulation of Plasma-sprayed Coatings. I. Coating Deposition Model, *Surf. Coat. Technol.*, 1991, **48**, p 137-145
5. D.E. Wroblewski, R. Khare, and M. Gevelber, Solidification Modeling of Plasma Sprayed TBC: Analysis of Remelt and Multiple Length Scales of Rough Substrates, *J. Therm. Spray. Technol.*, 2002, **11**(2), p 266-275
6. Y. Heichal and S. Chandra, Predicting Thermal Contact Resistance Between Molten Metal Droplets and a Solid Surface, *J. Heat Transfer*, 2005, **127**, p 1269-1275
7. R. Ghafouri-Azar, J. Mostaghimi, S. Chandra, and M. Charmchi, A Stochastic Model to Simulate Formation of a Thermal Spray Coating, *J. Therm. Spray. Technol.*, 2003, **12**, p 53-69
8. M. Pasandideh-Fard, S. Chandra, and J. Mostaghimi, A Three-Dimensional Model of Droplet Impact and Solidification, *Int. J. Heat Mass Transfer*, 2002, **45**, p 2229-2242